Int. J. Electrochem. Sci., 13 **(2018)** 4208 – 4222, doi: 10.20964/2018.05.41

International Journal of
ELECTROCHEMICAL
SCIENCE
www.electrochemsci.org

Electrochemical Studies on the Reduction Behavior of Co^{2+} in Eutectic NaF-KF Melt

Ming Li[1], *Xiaoli Xi*[2,*], *Zuoren Nie*[3], *Liwen Ma*[3], *Qingqing Liu*[3]

College of Material Science and Engineering, Beijing University of Technology, Beijing 100124, China
[*]E-mail: xixiaoli@bjut.edu.cn

Received: 4 January 2018 / *Accepted:* 4 March 2018 / *Published:* 10 April 2018

In this work, the electrochemical behavior of cobalt ion was investigated using an inert graphite rod electrode at 1073 K in NaF-KF-CoF_2 (1 wt%) molten salt system. Several transient electrochemical techniques, such as cyclic voltammetry, square wave voltammetry, and chronopotentiometry, were used. Results showed that electroreduction of Co^{2+} to Co is a reversible, one-step, two-electron transfer. The diffusion coefficient of Co^{2+} was investigated with cyclic voltammetry, square wave voltammetry, and chronopotentiometry, and results from the considered methods exhibited fair agreement. Electrodeposition of cobalt was performed at -0.3 V versus Pt at 1073 K for 4 h in a NaF-KF-CoF_2 (1 wt%) melt. The deposits were examined using X-ray diffraction and X-ray fluorescence, and results confirmed the obtained deposits as metallic cobalt. The present study aims to provide a theoretical reference for electrolysis of WC-Co hard metal scraps in molten salt.

Keywords: Cobalt, Molten salts, Electrochemistry, Diffusion coefficient.

1. INTRODUCTION

Cobalt is known as a strategic and critical metal considering its numerous industrial applications [1]. Application of cobalt metal mainly concentrates on rechargeable batteries and in the manufacture of corrosion and wear-resistant alloys. Other major uses of this metal include the manufacture of catalysts for petroleum and chemical industries, as a drying agent for paint varnishes, and ground coats for porcelain enamels, magnetic recording media, and steel-belted radial tires [2]. Thus, electrodeposition and electrochemical behavior of cobalt have received much attention because of wide spread cobalt application.

In recent years, given the low current efficiency and poor deposit quality due to hydrogen embrittlement, fewer people investigate the electrodeposition of cobalt and electrochemical behavior

cobalt ions in aqueous electrolytes. By contrast, molten salts were considered ideal electrolytes owing to numerous advantages, including a wide electrochemical window, high operating temperature range, and desirable ion conductivity in electrolysis without hydrogen gas generation [3, 4]. Given such properties, more people investigate cobalt ion electrochemical behavior and electrodeposition in molten salts. Electrodeposition behavior of cobalt ion was first studied in room-temperature molten salts (ionic liquid). Carlin et al. [5, 6] have reported the electrochemical reduction of cobalt from chloroaluminate ionic liquid. They observed that pure cobalt deposition proceeds via three-dimensional (3D) progressive nucleation with diffusion-controlled growth. An [7] et al. have reported the electrochemical behavior and electrodeposition of cobalt from $ZnCl_2$-EMIC-$CoCl_2$ ionic liquid. They also observed that electrodeposition of cobalt on tungsten electrode is governed by progressive 3D nucleation and diffusion-controlled growth mechanisms. At 373 K, the average diffusion coefficient of Co (II) in the melt reaches 1.1×10^{-6} cm2 $\cdot s^{-1}$. Chen et al. [8] have studied the electrodeposition of cobalt on nickel electrode from zinc chloride-1-ethyl-3-methylimidazolium chloride ionic liquid. They observed that cobalt deposition occurs via instantaneous 3D nucleation with diffusion-controlled growth of nuclei. Tulodziecki et al. [9] stressed the significance of the appearance of an electric double-layer structure in electrochemical deposition of cobalt from ionic liquid containing soluble Co^{2+}. The authors revealed in-depth the mechanism of Co^{2+} electroreduction on the electrode surface at elevated temperature. They also observed that the reaction rate dropped sharply with a well-shaped reduction peak during oxidation sweep. These phenomena were due to the reconstruction of the electric double-layer structure. Katayama et al. [10] studied the effects of temperature and additives on cobalt electrodeposition in imide-type room-temperature ionic liquid. Result indicated that elevated temperature can significantly reduce the overpotential of cobalt electrodeposition. Addition of acetone can decrease the overpotential of cobalt electrodeposition, implying that charge transfer rate is controlled by selective coordination of Co cations. All these results illustrated that coordination of cobalt ion and the appearance of electric double-layer structure can influence charge transfer and crystal growth in ionic liquids. Recently, some authors studied the electrochemical behavior of cobalt ion from high-temperature molten salts. Park [11] et al. investigated the electrochemical behavior of Zr, Sn, Fe, Cr, and Co in LiCl-KCl melt with cyclic voltammetry. They observed that electroreduction of cobalt ion proceeds in one step with two electrons, and is controlled by diffusion. Xi [12, 13] et al. studied the electrochemical behavior and electrodeposition of cobalt during electrolysis of hard metal scraps. They discovered that electroreduction of cobalt ion dissolved from WC-10Co hard metal scrap occurred through a one-step process involving the transfer of two electrons, indicating that the electrochemical behavior of cobalt ion is a diffusion-controlled reversible process. Although electrodeposition and electrochemical behavior of cobalt ion have been studied in many papers, few studies reported cobalt ion electroreduction and electrodeposition behavior in high-temperature molten salts. Some basic data on cobalt ion electroreduction behavior in high-temperature molten salt also remain lacking.

In this study, reduction/oxidation mechanism of Co was investigated in NaF-KF eutectic melt. CoF_2 was selected as the cobalt ion source. Transient electrochemical techniques, such as cyclic voltammetry, square wave voltammetry, and chronopotentiometry, were applied to investigate the typical redox potentials of cobalt ion, reversibility of electrode reactions, and diffusion coefficient of

cobalt ions in the molten melt. The present study aims to provide a theoretical reference for the electrolysis of WC-Co hard metal scraps in molten salt.

2. EXPERIMENTAL METHODS

All electrochemical experiments were carried out in a three-electrode system assembled in a graphite crucible, which was placed within the constant-temperature zone of a stainless vessel and heated in an electric furnace. The experimental set-up used in this work was described in detail in the previous publication of our group [14]. The temperature during experiment was measured with a Pt-Rh thermocouple with an accuracy of ±2 K and maintained at 1073 K by a proportional integral-derivative thermal controller. The inert experiment atmosphere was achieved with continuous circulation of argon gas at 99.99% purity.

The utilized analytic electrochemical techniques required a three-electrode set-up. Two graphite rods (Φ3 mm) were utilized as the working electrode and count electrode for electrochemical behavior investigation during the entire electrolytic process. A platinum wire (Φ0.5 mm) was selected as a quasi-reference electrode Pt/PtOx/O^{2-}, due to its corresponding inertness with respect to metal ions in molten salts [15]. The electrodes were cleaned by polishing with fine abrasive paper and washing ultrasonically in distilled water and anhydrous ethanol before use.

All the chemical reagents employed in this study were of analytical grade. The mixture of NaF-KF with eutectic composition (39.7%:60.3%) served as the supporting electrolyte, previously dehydrated at 573 K for 24 h, and pre-melted at 1073 K for the removal of residual moisture. The pre-melted salt mixture was melted again at 1073 K for the main experiment. Cobalt ions were introduced into the melt in the form of CoF_2 (1 wt%). The electrodes were inserted in the molten melt with an immersion area of 0.82 cm^2 for the working electrode. Sufficient equilibrium between the electrode and molten salt was guaranteed by immersing the electrodes in the melt for more than 2 h before electrochemical measurements.

All electrochemical measurements were carried out with PARSTAT 4000 electrochemical working station, along with the Versa Studio software package (Advanced Measurement Technology, Inc., USA). Transient electrochemical techniques, including cyclic voltammetry, square wave voltammetry, and chronopotentiometry, were used to study the electrochemical behavior of Co^{2+} in the molten salt. Cathode products were analyzed by X-ray diffraction (XRD) and X-ray fluorescence (XRF).

3. RESULTS AND DISCUSSION

3.1 Cyclic voltammetry

To investigate the electroreduction behavior of Co^{2+} in the melts more accurately, the cyclic voltammogram of blank NaF-KF melt was obtained to primarily confirm the electrochemical window. Fig. 1 shows the cyclic voltammogram obtained in blank NaF-KF melts on the inert graphic electrode at 1023 K.

Peaks R0 and O0 corresponded to the intercalation and inlaying of sodium ion on graphite electrode [16]. Fig.1 displays that the blank NaF-KF melts exhibited high stability in electrochemical window between -0.6 V to 0.8 V versus Pt electrode owing to the absence of reduction peaks within such range. Trace impurities in blank NaF-KF melts showed no effects on analysis results.

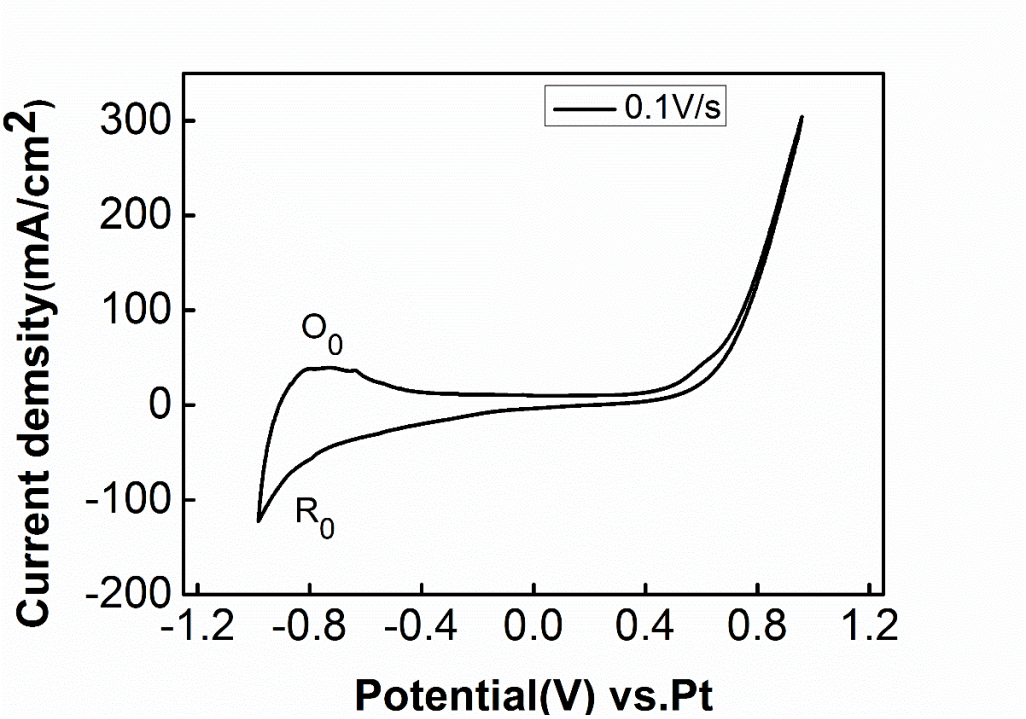

Figure 1. Cyclic voltammogram for a graphic rod electrode in molten NaF-KF eutectic at 1073 K. (Temperature: 1073 K; Working electrode area: 0.82 cm^2).

Cyclic voltammograms of NaF-KF-CoF_2 (1 wt%) systems with the scan rate of 0.1 V/s for the graphite rod electrode were recorded at 1073 K, as depicted in Fig. 2. With Co ions in the molten melt, Fig.2 shows one cathodic peak R1 at -0.25 V versus Pt, and the corresponding anodic peak O1 was observed at 0.28 V, when the potential was swept back to the positive side. A crossover was detected at -0.3 V versus Pt from onset potential to negative scan, and this result was attributed to the appearance of cobalt metal phase [17].

At a fixed potential, cyclic voltammetric results of NaF-KF-CoF_2 (1% wt) melt from -0.4 to 0.4 V versus Pt at varying scan rates, as shown in Fig. 3. The redox peaks R1 and O1 were evident in the cyclic voltammetry curves. In general, the peak currents of redox peaks increased with increasing scan rate. For the cathodic process, peak potentials of R1 moved insignificantly to the negative side with a potential change of 40 mV, when the scan rate was increased from 0.2 V/s to 0.5 V/s; results indicate that reduction of Co(II)/Co is reversible(or quasi-reversible)[18].

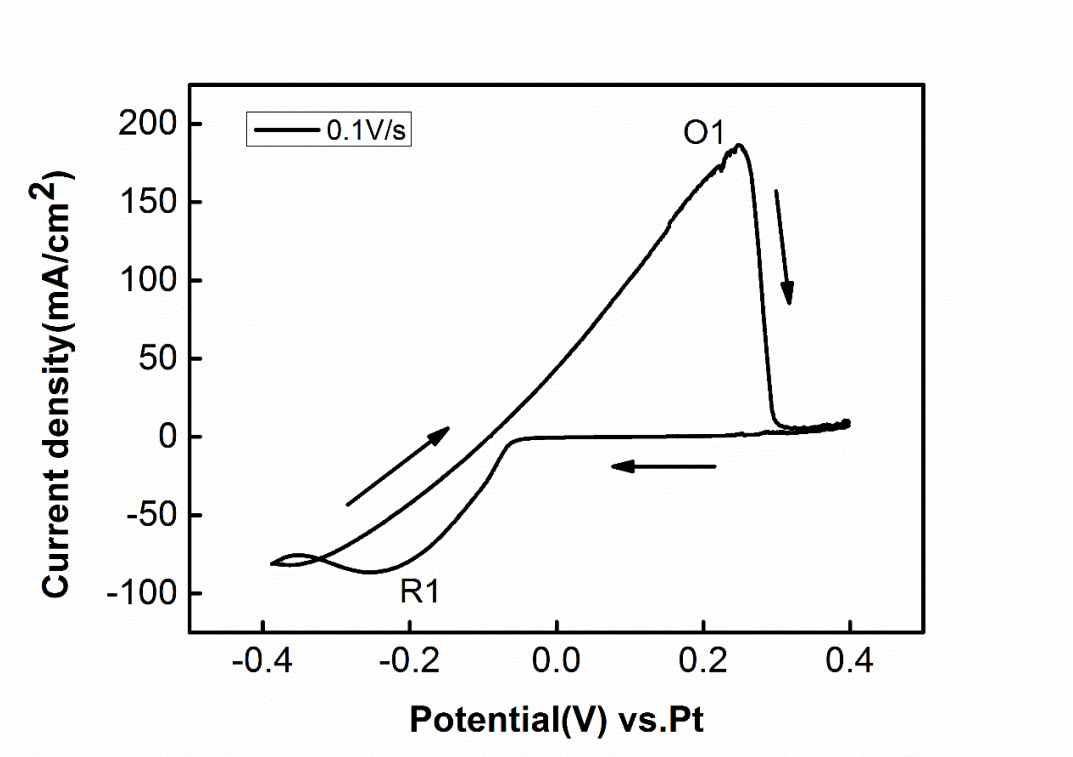

Figure 2. Cyclic voltammogram of Co^{2+} for the graphic rod electrode in molten NaF-KF-CoF_2 eutectic at 1073 K. (Temperature: 1073 K; Working electrode area: 0.82 cm^2).

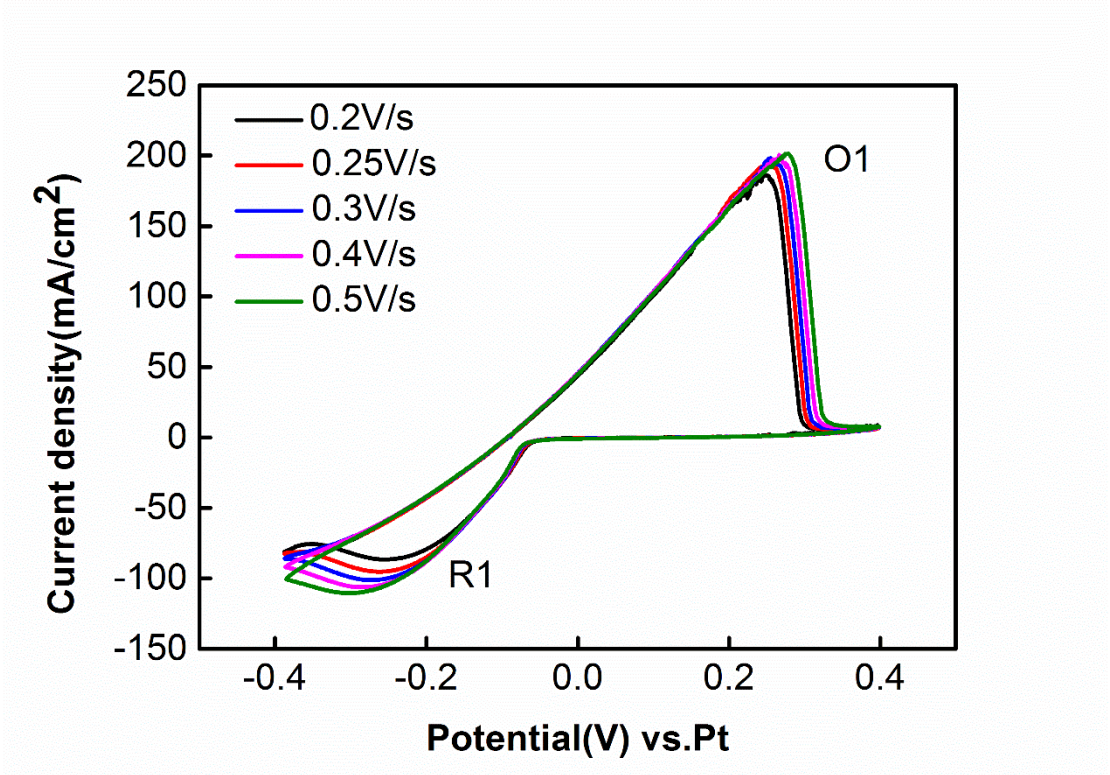

Figure 3. Cyclic voltammograms at various scan rates for the graphic rod electrode in molten NaF-KF-CoF_2 (1%wt) eutectic at 1073 K. (Temperature: 1073 K; Working electrode area: 0.82 cm^2).

According to Bard and Faulkner [19], the following equation can calculate the number of exchanged electrons by the relationship between peak potential, half peak potential, and the number of electrons transferred; such relationship is suitable for reversible systems:

$$E_p - E_{\frac{P}{2}} = -\frac{2.2RT}{nF} \qquad (1)$$

Where E_p is the peak potential, and $E_{p/2}$ represents the half-peak potential.

In electroreduction of Co^{2+} to Co, the number of exchanged electrons was determined to be 2 by the above equation(Table.1). Results suggest that reduction process of Co(II) is a reversible process with two electrons.

Table 1. Obtained data of cyclic voltammograms at various scan rates.

Scan rate(V/s)	E_p	$E_{p/2}$	n
0.2	-0.249	-0.151	2.07
0.25	-0.260	-0.156	1.96
0.3	-0.270	-0.161	1.87
0.35	-0.280	-0.166	1.78
0.4	-0.300	-0.181	1.71
Average			1.88

Fig.4 shows the relationship between scan rate and peak potential /current for the cathodic reactions. Fig.4 (a) illustrates that the shift in peak potential for the electrode reaction at R1 with the increase of scan rate from 0.2 V/s to 0.5 V/s, indicating the reversibility of the cathode process. The liner dependence of peak current of R1 on the square root of scan rates represented in Fig.4 (b) reflects a diffusion-controlled mass transfer for the cathodic process.

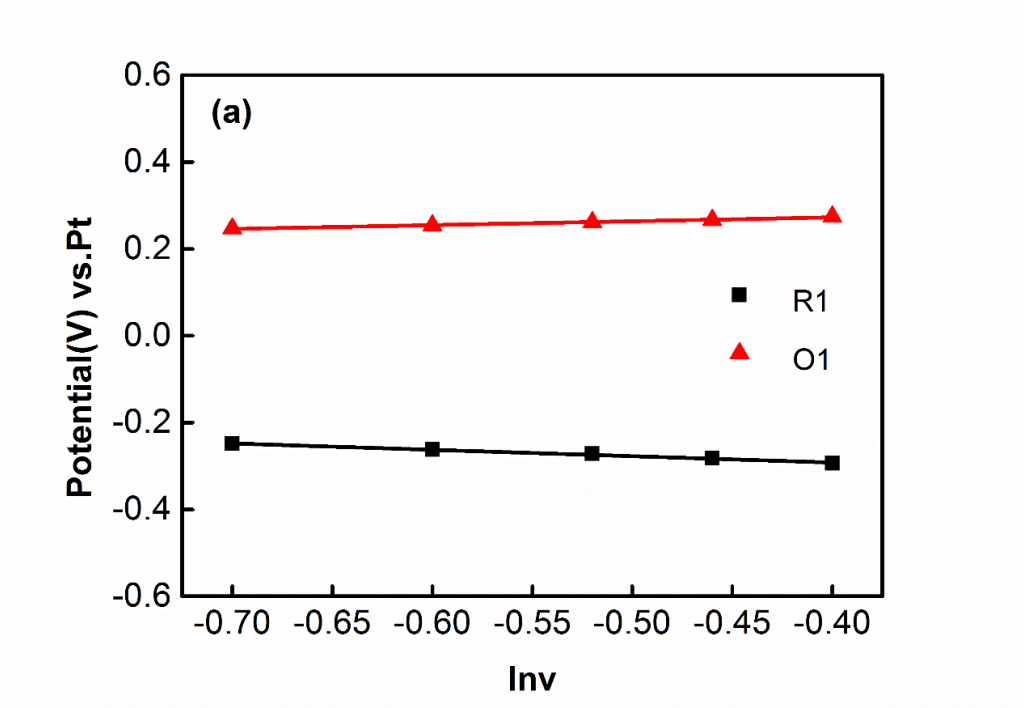

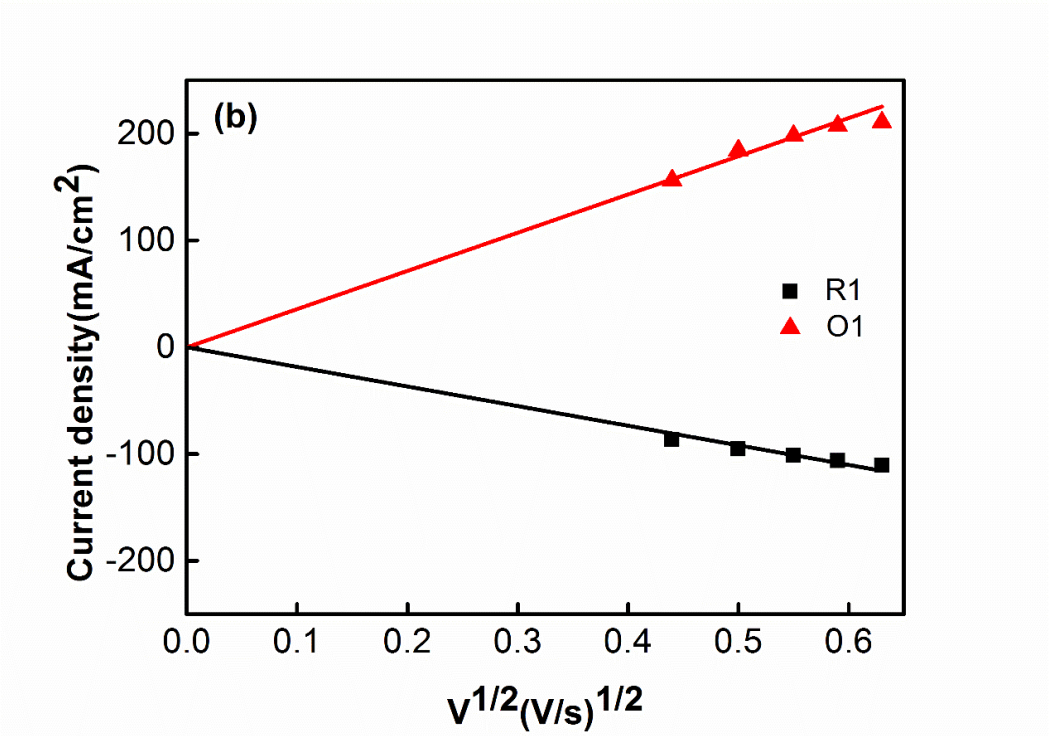

Figure 4. (a) Dependence of peak potential on natural logarithm of scan rates. (b) Dependence of peak current on square root of scan rate. (Working g electrode area: 0.82 cm^2).

For diffusion-controlled electrochemical reactions of reversibility, the diffusion coefficient of Co ions in the molten salt can be estimated with Randles-Shevchik equation, as shown in Eq.2 [19]:

$$I_p^c = 0.4463(nF)^{3/2}(RT)^{-1/2}C_0^* v^{1/2} AD^{1/2} \quad (2)$$

where *A* refers to the immersion area of the graphite rod working electrode (cm^2), n represents the number of exchanged electrons, *F* is Faraday constant (96485C/mol), *R* corresponds to the molar gas constant (8.314 J/mol·K),*T* is temperature (K), *D* denotes the diffusion coefficient of Co ion(cm^2/s), *C* stands for the molar concentration of Co ions (mol/cm^3),and *v* is the scan rate(V/s).

According to the relationship of diffusion coefficient with the peak currents at various scan rates, at the temperature range of 1023 K to 1123 K, the diffusion coefficient of Co(II) ions in the molten NaF-KF-CoF_2(1wt%) system were evaluated based on Eq.(2),as to be within the range of 2.88 $\times 10^{-6}$ cm^2/s to 3.77$\times 10^{-6}$ cm^2/s .

The influence of temperature on the value of diffusion coefficient of Co(II) was determined by plotting lnD versus the reverse of absolute temperature(shown in Fig. 5).A straight line was obtained, and it showed the validity of the Arrhenius law in reduction of Co(II) (expressed as Eq.(3))[19]:

$$D=Ae^{\left(\frac{-E_\alpha}{RT}\right)} \quad (3)$$

Where *A* refers to the pre-exponential factor, E_α is activation energy (KJ/mol), and *T* denotes the absolute temperature. Finally, the diffusion coefficient of Co (II) was formulated as follows:

$$\ln D = -9.75 - \frac{3076}{T} \quad (4)$$

Table 2. Experimental value of D of Co (II) species at different temperatures.

Temperature (K)	1023	1048	1073	1098	1123
D($\times10^{-6}$ cm^2/s)	2.88	3.11	3.30	3.73	3.77

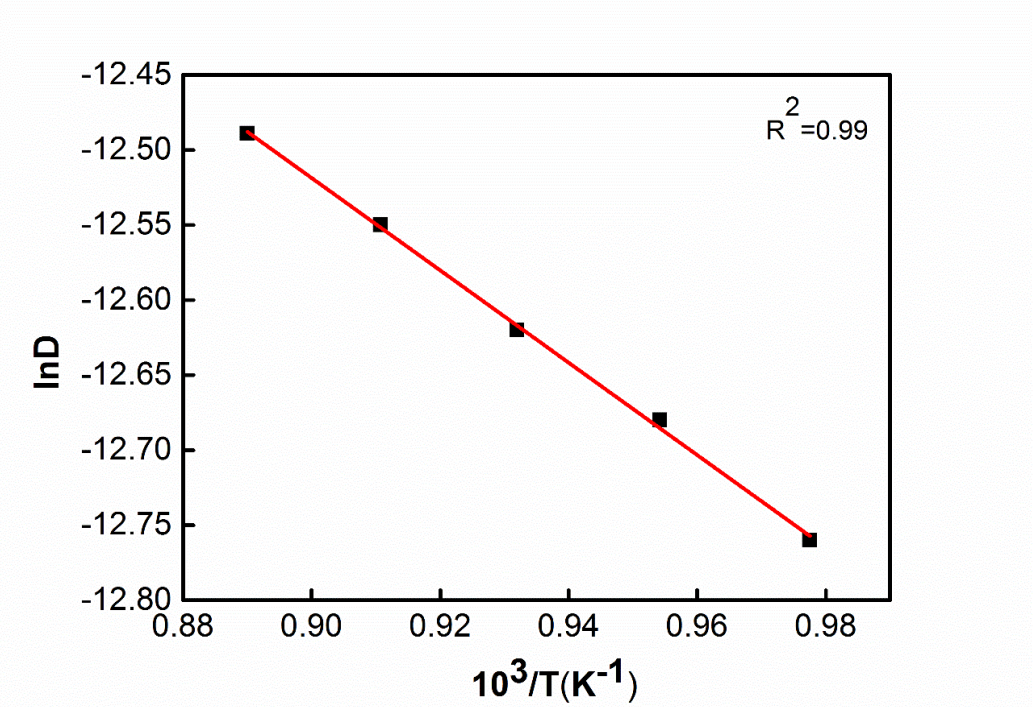

Figure 5. Variation in diffusion coefficient of Co (II) in NaF-KF molten salt with increasing temperature.

From this equation, temperature dependence of diffusion coefficient was established, and activation energy value for the diffusion process can be extracted (E_α=-25.57 kJ/mol), this result was independent of temperature. The pre-exponential term A was calculated to be 5.83×10^{-5} cm^2/s.

3.2 Square wave voltammetry

A more sensitive transient electrochemical technique , square wave voltammetry [20,21] was carried out to further investigate the electrochemical behavior of cobalt ion in NaF-KF eutectic.Fig.6(a) shows the typical square wave voltammetry of NaF-KF-CoF_2 (1 wt%) system with signal frequency varying from 10 Hz to 25 Hz. Results showed that a distinct reduction wave appeared at a potential of -0.2 V versus Pt, and this result is attributed to one-step reduction of cobalt ion. Eq. (5) gives the relationship between the half-width of the peak and the number of transferred electrons for n value estimation; this relationship is valid for reversible electrochemical systems.

$$W_{1/2} = \frac{3.52RT}{nF} \qquad (5)$$

Where *n* refers to the exchanging electron number, *R* is the ideal gas constant, *T* is absolute temperature, and *F* stands for Faraday constant.

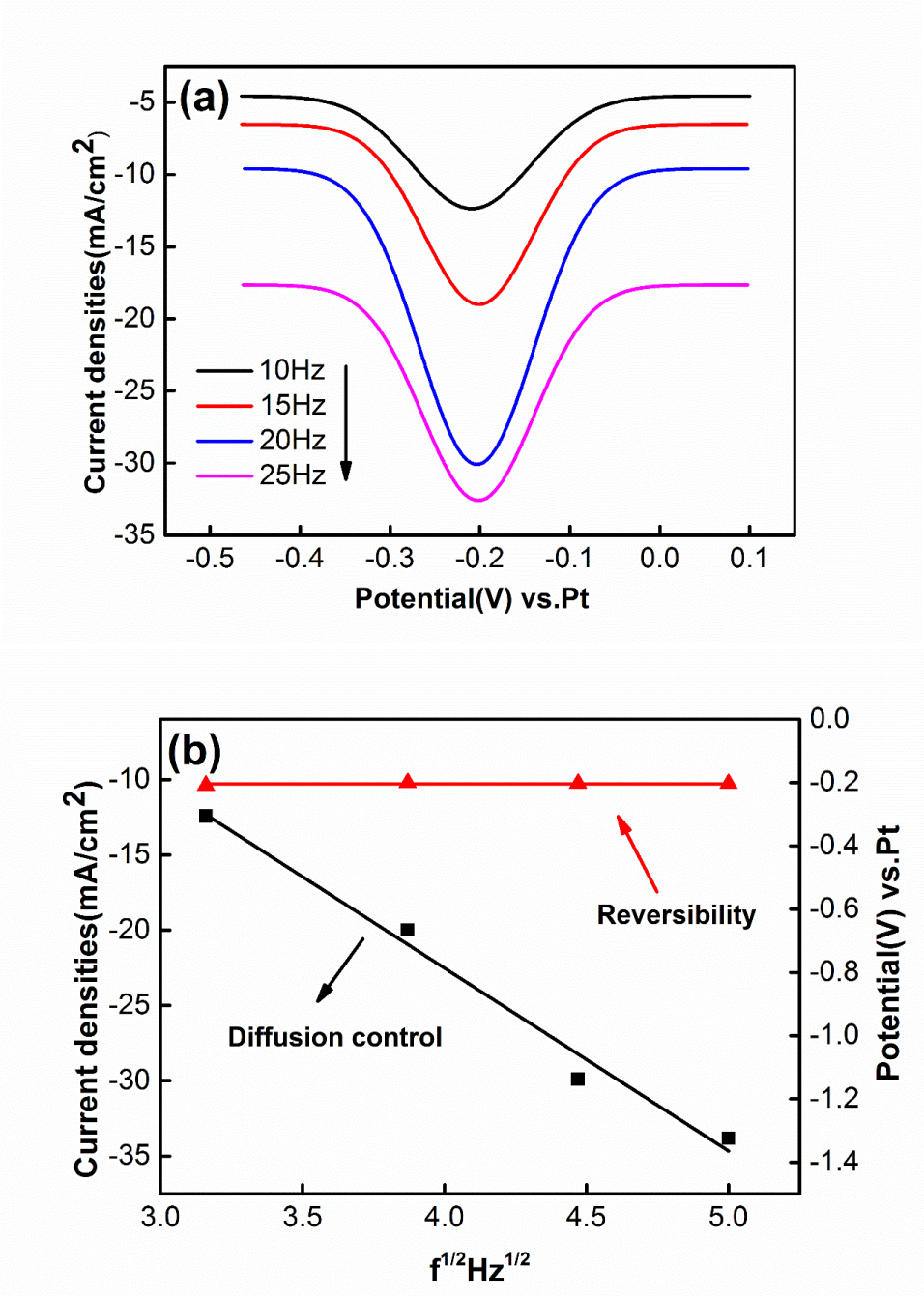

Figure 6. Square wave voltammogram of CoF_2 in NaF-KF melt on graphic rod electrode at 1073K. (Working electrode area: 0.82 cm^2, frequency: 10-25 Hz). (b) Linear relationship of the cathodic peak current (black line) and reduction peak R1 potential (red line) versus the square root of frequency.

The shape of R1 is symmetrical in nature. The numbers of transferred electrons ,which were evaluated based on Eq.5, reached 2.25, 2.16, 2.22 and 2.07 by width measurement at the mid-height of peak at various frequencies of a square wave signal (Table 3). These results confirm that the number of

electrons transferred is close to 2, and electroreduction of cobalt ions in the melt proceeded in one step with two exchanged electrons.

According to Li [14], the peak height and frequency square root were indicated by linear relationship, as presented in Fig.6 (b). Reversibility could be confirmed by the maximum current plot of the current peak versus the square root of frequency of the square wave signal. The obtained straight lines confirmed that reduction of Co (II)/Co (0) is a diffusion-controlled process. As the cathodic peak R1 remained constant over a specific frequency range, reduction of cobalt ion was a reversible process. This result was consistent with cyclic voltammetry results.

Table 3. Data on square wave voltammetry for R1

Frequency (Hz)	Half width (V)	Transferred electrons
10	0.144	2.25
15	0.150	2.16
20	0.146	2.22
25	0.157	2.07

3.3 Chronopotentiometry

To further investigate the electroreduction mechanism of Co^{2+}, typical chronopotentiograms of NaF-KF-CoF_2（1 wt%）melt with various applied current densities on the graphic rod electrode were obtained at 1073K. Fig.7 (a) shows the evolution of chronopotentigrams with the applied current densities from 73.17 mA/cm^2 to 103.66 mA/cm^2. Transition time τ corresponds to peak R1 of the cyclic voltammetry. The potential of the platform in chronopotentiometric curves showed no movement in the negative direction with increasing current densities. This result further suggested that electrochemical reduction of Co (II) to Co should be a reversible electrochemical process.

The plateau evidenced at much more negative potential region represents the intercalation of alkali metal ions. In general, transition time decreased with increasing applied current densities, further confirming that the reduction of cobalt ion is a diffusion-controlled process. The time-current relationship for a diffusion-controlled electron transfer process is given by Sand`s law for the diffusion coefficient evaluation of Co ions in the melt, as calculated in Eq. (6) [19].

$$i\tau^{1/2} = \frac{nFAC_0\pi^{1/2}D^{1/2}}{2} \quad (6)$$

The diffusion coefficient of Co(II) in the NaF-KF-CoF_2 melt at 1073 K, as evaluated with Eq.(6) , ranged from 8.03×10^{-6} cm^2/s and 4.95×10^{-6} cm^2/s (Table 4) ,and this result agrees well with the data obtained by cyclic voltammetries . The diffusion coefficient of Co(II) (approximately 2.5×10^{-6} cm^2/s) evaluated in the present study accords closely with the corresponding results estimated by Yang et al. in the molten urea-NaBr-KBr-$CoCl_2$ at 373 K [22]; Li et al. yielded a result of 1.7×10^{-6} cm^2/s in molten urea-chloline-chloride-$CoCl_2$ at 373 K [4]; Li et al. obtained a value of 2.2×10^{-6} cm^2/s in molten urea-acetamide-LiBr-$CoCl_2$ at 353 K[3].

For a reversible process, the potential-time relationship is presented by Eq. (7) [19]. Fig.7 (b) shows the relationship between potential and transition time. From the slope of plot E versus ln

$\{(\tau^{1/2} - t^{1/2})/t^{1/2}\}$, the transferred electron value "n" was calculated for cobalt ion in molten NaF-KF eutectic on graphite electrode. The calculated value of "n" totaled 2.05 at 1023 K, indicating that electroreduction of cobalt ion in the melt proceeded in one step with two exchanged electrons.

$$E = E_{\tau/4} + \frac{RT}{nF} ln\left\{\frac{\tau^{1/2} - t^{1/2}}{\tau^{1/2}}\right\} \quad (7)$$

Where n represents the exchanging electron number, R is the ideal gas constant, T is absolute temperature, F is Faraday constant and τ denotes transition time.

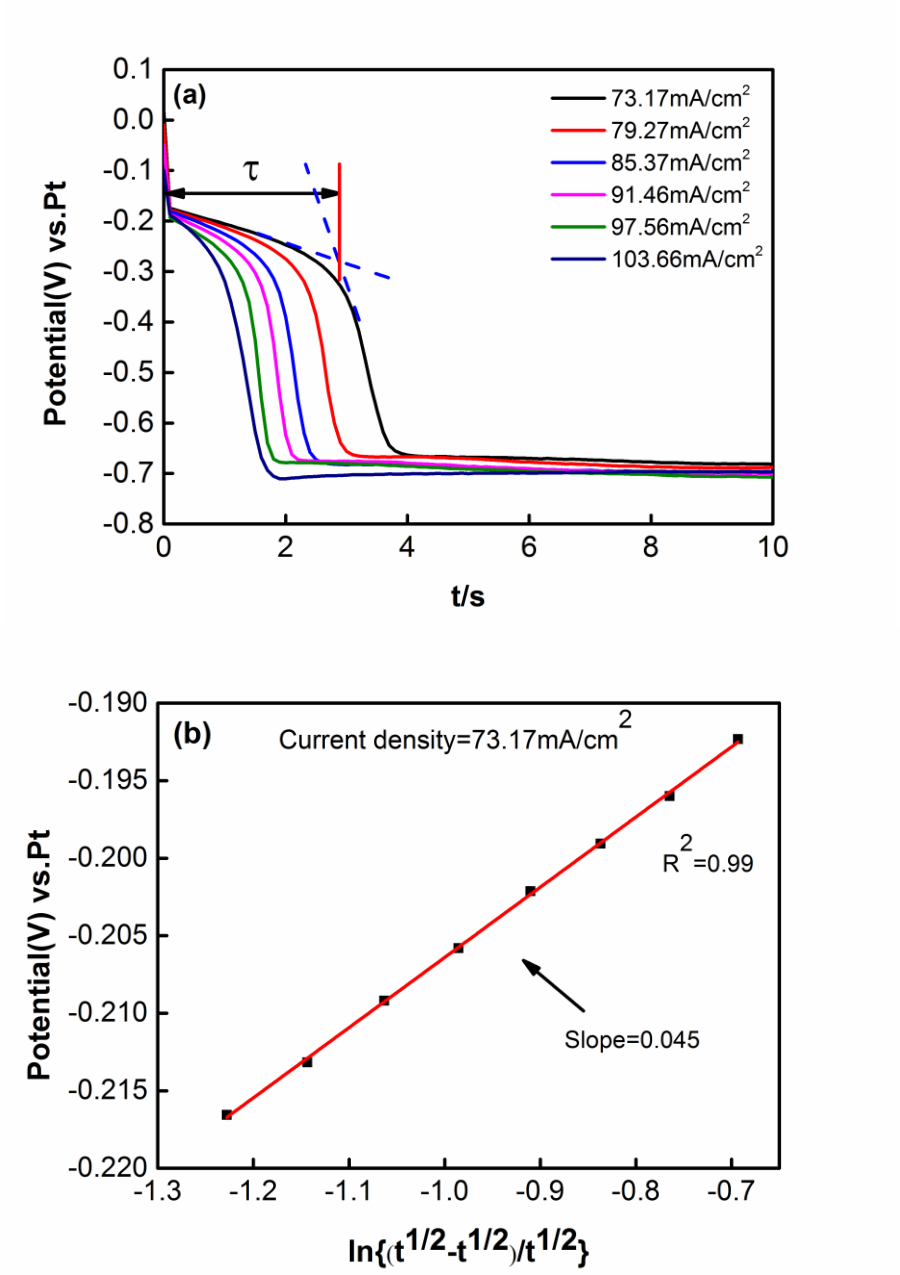

Figure 7. (a) Chronopotentiograms of the NaF-KF-CoF_2(1 wt%) system at 1073 K with varing applied current densities. (Working electrode area: 0.82 cm^2). (b) Logarithmic analysis of chronopotentiogram at current density 73.17 mA/cm^2.

Table 4. Experimental value of D of Co (II) species at various current densities.

Current densities(mA/cm^2)	Transition time (s)	D(×10^{-6}cm^2/s)
73.17	2.8	8.03
79.27	2.25	7.57
85.37	1.87	7.30
91.46	1.62	7.26
97.56	1.36	6.93
103.66	0.86	4.95
Average		7.0

Fig.8 shows the current reversal chronopotentiograms for the graphic rod electrode at various current densities. An anodic plateau corresponding to the cathodic electrode was identified after the current reversal for each applied current density on the electrode. Anodic and cathodic transition time almost equal to each other, approximating 5.1, 2.96, 2.04, 1.54 and 1.05s at electrode currents of ± 50, ± 60, ± 70, ± 80 and ± 90 mA, respectively. The equality of transition time indicates the deposition and dissolution of an insoluble compound during the cathodic and anodic processes, further confirming that metallic Co was formed on the electrode through reduction reaction of Co (II)/Co at about -0.2 V versus Pt.

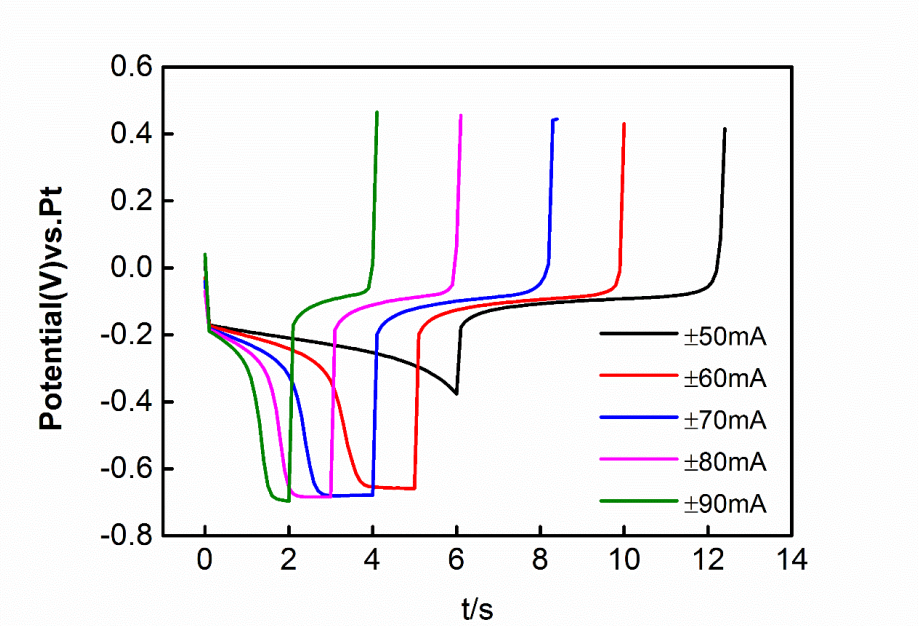

Figure 8. Current reversal chronopotentiograms of the NaF-KF-CoF_2 (1 wt%) system at 1073K with varing applied currents. (Working electrode area: 0.82cm^2).

3.4 Characterization of cathodic products

After the electrochemical tests of cobalt ion in NaF-KF melt, potentiostatic electrolysis was performed at a potential of -0.3 V versus Pt, as presented in Fig.2, to deposit cobalt metal in NaF-KF-CoF_2 (1 wt%) melt.

Table 5. Results of chemical analysis from XRF

Element	Co	Na	K
Mass (%)	97.65	0.88	1.47

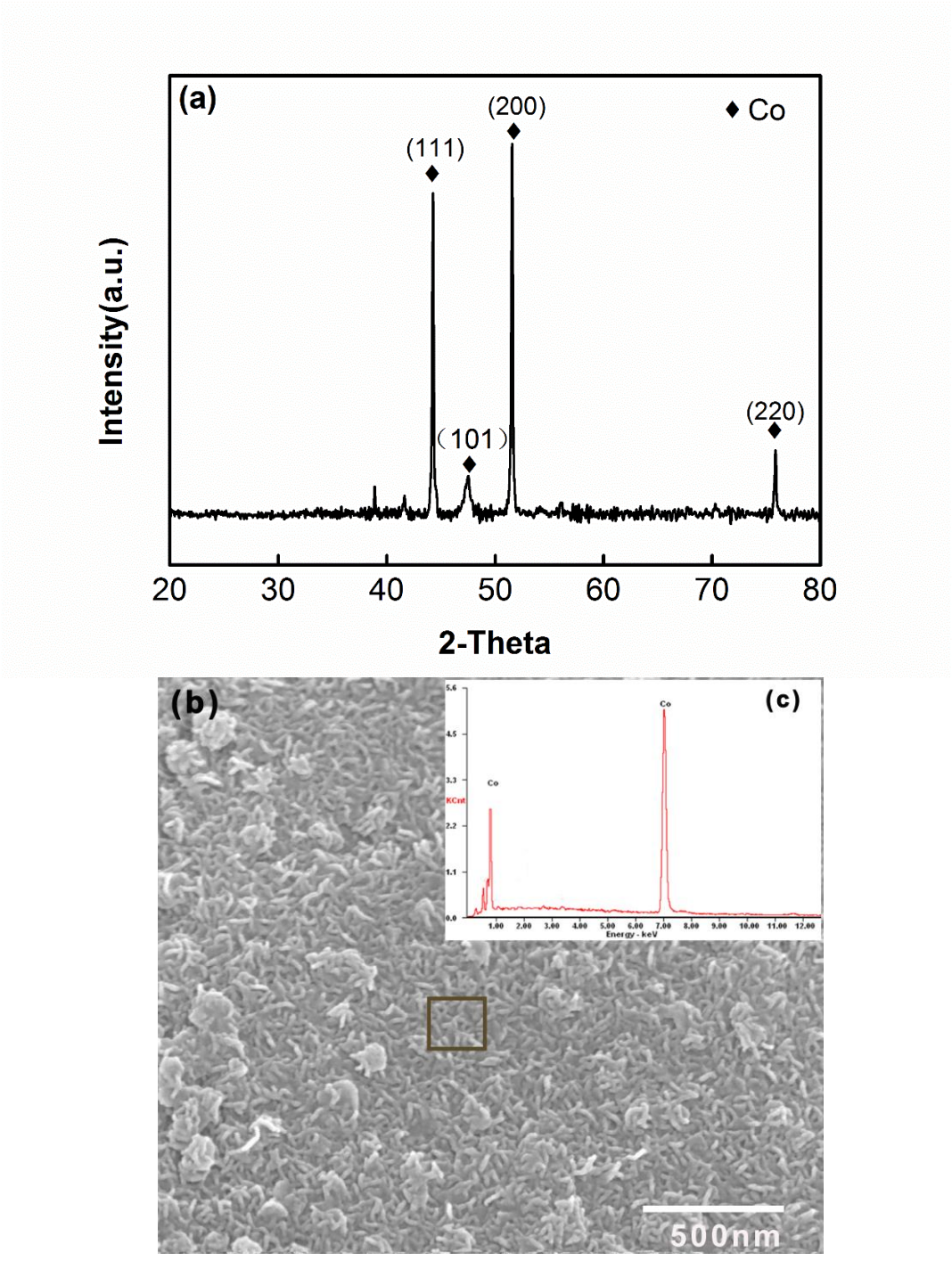

Figure 9. (a) XRD pattern (-0.3 V vs.Pt) of cathodic product after potentiostatic electrolysis in NaF-KF-CoF_2 (1 wt%) melt on an inert graphic rod electrode at 1073 K. (b) SEM image of cathodic product after potentiostatic electrolysis of NaF-KF-CoF_2 (1 wt%) melt on an inert graphic rod electrode at 1073 K. (c) EDS spectrum of cathodic product.

Fig.9 (a) shows the XRD patterns of cathode products after electrolysis. Results showed that the electrolysis product obtained at the cathode was cobalt metallic powder matching with the hexagonal close-packed standard cobalt. Fig.9 (b) and Fig.9 (c) shows the SEM image of the cobalt deposits obtained from NaF-KF-CoF_2 (1 wt%) melt at potentiostatic electrolysis, the results indicates that the cobalt wire was obtained. According to Yi [23], the appearance of cobalt wire was attributed to the involvement of cobalt electrodeposition with the instantaneous 3D nucleation and growth. All nuclei were born and grew simultaneously. XRF was also applied to investigate the purity of cathode product. Purity of cathode products reached 97.65 %(Mass %) with low levels of sodium and potassium, as shown in Table 5. Trace impurities can be due to the adhesion of NaF-KF melts. Thus, cobalt metal can be availably produced from NaF-KF-CoF_2 (1 wt%) melt by the graphic cathode.

4. CONCLUSIONS

The electrochemical behavior study of Co^{2+} ions in the eutectic NaF-KF molten salt system on an inert graphic rod electrode was investigated by several electrochemical techniques at 1073 K. Results showed that electrochemical reduction of cobalt ion was controlled by diffusion of ions from electrolyte to electrode interface. The diffusion coefficient of cobalt ion in the melt measured 3.3×10^{-6} cm^2/s by cyclic voltammetry, and approximated 7.0×10^{-6} cm^2/s through chronopotentiometry. The results obtained by the considered methods showed good agreement.

Deposition process of cobalt ions on graphic rod electrode involves a one-step reaction with the exchange of two electrons. The cobalt metal was obtained at the cathode under potentiostatic electrolysis at a potential of -0.3 V versus Pt in NaF-KF-CoF_2 melt. Results of XRF indicated that purity of cobalt metal totaled 97.65 %(Mass %).

ACKNOWLEDGEMENTS
This research was financially supported by the National Natural Science Foundation of China (51422401 and 51621003) and Beijing Natural Science Foundation (2172010).

References

1. Minerals yearbook: Cobalt statistics and information, USGS (2013). http://minerals.usgs.gov/minerals/pubs/commodity/ cobalt/.
2. P. Patnaik , S.K. Padhy, B.C. Tripathy, I.N. Bhattacharya and R.K. Paramguru, *Trans. Nonferrous Met. Soc. China,* 25 (2015) 2047.
3. M. Li, B.L. Gao, Z.N. Shi, X.W. Hu, S.X. Wang, L.X. Li, Z.W. Wang and J.Y. Yu, *J. Solid State Electrochem.*, 20 (2016) 247.
4. M. Li, Z.W. Wang and G.R. Ramana, *Electrochim. Acta,* 123 (2014) 325.
5. T.R. Carlin, P.C. Trulove and H.C. Delong, *J. Electrochem. Soc.,* 143 (1996) 2747.
6. T.R. Carlin, H.C. Delong, J. Fuller J and P.C. Trulove, *J. Electrochem. Soc.,* 145 (1998) 1598.
7. A.M. Zhong, Y. Peixia, S. Caina, A. Nishikata and T. Tsuru, *Chin. Chin. J. Chem.,* 26 (2008) 1219.
8. C. Poyu and S. Iwen, *Electrochim. Acta,* 46 (2001) 1169.
9. M. Tulodziecki, J.M. Tarascon, P.L. Taberna and C. Guery, *Electrochim. Acta,* 134 (2014) 55.
10. Y. Katayama, R. Fukui and T. Miura, *J. Electrochem. Soc.,* 154 (2007) D534.

11. P. Jaeyeong, C. Sungyeol, S. Sungjune and H. Soon, *J. Electrochem. Soc.*, 164 (2017) D744.
12. X.L. Xi, Q.Q. Liu, Z.R. Nie, M. Li and L.W. Ma, *Int. J. Refract. Met. Hard Mater.*, 70 (2018) 77.
13. X.L. Xi, X.J. Xiao, Z.R. Nie, L.W. Zhang and L.W. Ma, *J. Electroanal. Chem.*, 794 (2017) 254.
14. M. Li, X.L. Xi, Z.R. Nie and Q.Q. Liu, *J. Electrochem. Soc.*, 163 (2016) D728.
15. L. Massot, P. Chamelot, L. Cassayre and P. Taxil, *Electrochim. Acta*, 54 (2009) 636.
16. G.Z. Chen, I. Kinloch, M.S. Shaffer and D.J. Fray, *High Temp. Mater. Processes (Danbury, CT, U. S.*, 2 (1998) 459.
17. K. Ghayoung, Y. Dalseong, P. Seungwoo, K.S. Hyung, K.T. Jin and A.D. Hee, *J. Electroanal. Chem.*, 682 (2012) 128.
18. C. Zeng, Y.J. Li and S.J. Li, *J. Alloys Compd.*, 509 (2011) 5958.
19. A.J. Bard and L.R. Faulkner. *Electrochemical Methods, Fundamentals and Applications* .John Wiley& Sons Inc, (1981) New York, America.
20. T. Hao, Y. D. Yan, M.L. Zhang, X. Li, Y. Huang, Y.L. Xu, Y. Xue, W. Han and Z.J. Zhang, *Electrochim. Acta*, 88 (2013) 457.
21. K. Liu, Y.L. Liu, L.Y. Yuan, X.L. Zhao, Z.F. Chai and W.Q. Shi, *Electrochim. Acta*, 109 (2013) 732.
22. Q.Q. Yang and K.R. Qiu, *Electrochemistry*, 3 (1995) 274.
23. Y.T. Hsieh, M.C. Lai, H.L. Huang and I.W. Sun. *Electrochim. Acta*, 117 (2014) 21.